

## BIROn - Birkbeck Institutional Research Online

Grey, W. and Chauhan, R. and Piganeau, M. and Huerga, E. and Garcia-Albornoz, M. and McDonald, Neil and Bonnet, D. (2020) Activation of the Receptor Tyrosine Kinase, RET, improves long-term Hematopoietic Stem Cell outgrowth and potency. *Blood* 136 (22), pp. 2535-2547. ISSN 0006-4971.

Downloaded from: <https://eprints.bbk.ac.uk/id/eprint/32542/>

*Usage Guidelines:*

Please refer to usage guidelines at <https://eprints.bbk.ac.uk/policies.html>

or alternatively

contact [lib-eprints@bbk.ac.uk](mailto:lib-eprints@bbk.ac.uk).



American Society of Hematology  
2021 L Street NW, Suite 900,  
Washington, DC 20036  
Phone: 202-776-0544 | Fax 202-776-0545  
editorial@hematology.org

## **Activation of the receptor tyrosine kinase, RET, improves long-term hematopoietic stem cell outgrowth and potency**

Tracking no: BLD-2020-006302R2

William Grey (The Francis Crick Institute, United Kingdom) Rakhee Chauhan (The Francis Crick Institute, United Kingdom) Marion Piganeau (The Francis Crick Institute, United Kingdom) Hector Huerga Encabo (The Francis Crick Institute, United Kingdom) Manuel Garcia-Albornoz (The Francis Crick Institute, United Kingdom) Neil McDonald (3. Institute of Structural and Molecular Biology, Department of Biological Sciences, Birkbeck College., United Kingdom) Dominique Bonnet (The Francis Crick Institute, United Kingdom)

### **Abstract:**

Expansion of Human Hematopoietic Stem Cells (HSCs) is a rapidly advancing field showing great promise for clinical applications. Recent evidence has implicated the nervous system and glial family ligands (GFLs) as potential drivers of hematopoietic survival and self-renewal in the bone marrow niche, but how to apply this to HSC maintenance and expansion is yet to be explored. We demonstrate a role for the GFL receptor, RET, at the cell surface of HSCs, in mediating sustained cellular growth, resistance to stress and improved cell survival throughout *in vitro* expansion. HSCs treated with the key RET ligand/co-receptor complex, GDNF/GFRa1, show improved progenitor function at primary transplantation and improved long-term HSC function at secondary transplantation. Finally, we demonstrate that RET drives a multi-faceted intracellular signalling pathway, including key signalling intermediates AKT, ERK1/2, NFkB and p53, responsible for a wide range of cellular and genetic responses which improve cell growth and survival under culture conditions.

**Conflict of interest:** No COI declared

**COI notes:**

**Preprint server:** No;

**Author contributions and disclosures:** W.G. designed and carried out experiments, analysed the data and wrote the manuscript. R.C., M.P., H.H.E & M.G-A. carried out experiments. N.Q.M. supervised the project. D.B. supervised the project and wrote the manuscript.

**Non-author contributions and disclosures:** No;

**Agreement to Share Publication-Related Data and Data Sharing Statement:** N/A

**Clinical trial registration information (if any):**

1     **Activation of the receptor tyrosine kinase, RET, improves long-term hematopoietic**  
2                                     **stem cell outgrowth and potency**

3     Grey, W.<sup>1</sup>, Chauhan, R.<sup>2</sup>, Piganeau, M.<sup>1</sup> Huerga Encabo, H.<sup>1</sup>, Garcia-Albornoz, M.<sup>1</sup>,  
4     McDonald, N.Q.<sup>2,3</sup>, Bonnet, D.<sup>1,4</sup>

- 5         1. Hematopoietic Stem Cell laboratory, The Francis Crick Institute.  
6         2. Signalling and Structural Biology laboratory, The Francis Crick Institute.  
7         3. Institute of Structural and Molecular Biology, Department of Biological Sciences,  
8             Birkbeck College.  
9         4. Corresponding Author: Dominique Bonnet, e:[dominique.bonnet@crick.ac.uk](mailto:dominique.bonnet@crick.ac.uk),  
10             t:+44(0)2037961198

11  
12     Abstract word count: 152

13     Text word count: 4,000

14     Number of figures: 6

15     Number of supplementary figures: 8

16     Number of references: 22

## 17 **Key Points**

- 18 • RET cell surface expression and activity is enriched in HSCs.
- 19 • Activation of RET by GDNF/GFR $\alpha$ 1 improves LT-HSC outgrowth *in vitro* and transplantation *in vivo*.

## 21 **Abstract**

22  
23 Expansion of Human Hematopoietic Stem Cells (HSCs) is a rapidly advancing field showing great promise for  
24 clinical applications. Recent evidence has implicated the nervous system and glial family ligands (GFLs) as  
25 potential drivers of hematopoietic survival and self-renewal in the bone marrow niche, but how to apply this to  
26 HSC maintenance and expansion is yet to be explored. We demonstrate a role for the GFL receptor, RET, at the  
27 cell surface of HSCs, in mediating sustained cellular growth, resistance to stress and improved cell survival  
28 throughout *in vitro* expansion. HSCs treated with the key RET ligand/co-receptor complex, GDNF/GFR $\alpha$ 1,  
29 show improved progenitor function at primary transplantation and improved long-term HSC function at  
30 secondary transplantation. Finally, we demonstrate that RET drives a multi-faceted intracellular signalling  
31 pathway, including key signalling intermediates AKT, ERK1/2, NF $\kappa$ B and p53, responsible for a wide range of  
32 cellular and genetic responses which improve cell growth and survival under culture conditions.

## 34 **Introduction**

35  
36 Hematopoietic stem cells (HSCs) are highly potent stem cells of the blood system, known to reside in the bone  
37 marrow of adults and umbilical cord blood (UCB) during pregnancy. Whilst bone marrow biopsy is invasive  
38 and harsh, collection of UCB represents a less invasive, clinically important source of HSCs and progenitors  
39 (HSPCs) for treatment of a wide range of malignant and non-malignant disorders. UCB has a lower incidence of  
40 graft versus host disease, with less stringent donor cross-matching required compared to classical donor sources,  
41 increasing its value for both hematological and non-hematological malignancies<sup>1</sup>. Despite increasing UCB  
42 banking, limited progenitor cell dose<sup>2</sup>, delay of engraftment and immune reconstitution<sup>3</sup> and the cost of double  
43 UCB transplantation in adults<sup>4</sup>, underline a need to improve expansion and potency of these cells for the  
44 purposes of transplantation.

45 To address these limitations, critical advances have been made in both identification and successful outgrowth  
46 of HSCs from bone marrow and UCB sources<sup>5-11</sup>. Despite these advances, further expansion of HSCs is  
47 required to address clinical issues associated with delayed engraftment/immune reconstitution, and relative  
48 paucity of HSCs produced at the end of current culture protocols.

49 In recent years, there has been increasing evidence that the nervous system may be important for  
50 communication with, and influence over, the hematopoietic system. Central to this theory, the receptor tyrosine  
51 kinase, RET, has been demonstrated to be expressed in murine HSCs, playing an important role in their survival  
52 *in vivo*, and potentiating outgrowth *in vitro* when activated by glial derived neurotrophic factor (GDNF) family  
53 ligands and co-receptors, mediating *Bcl2* expression<sup>12</sup>. These findings indicate that neuronal signals are  
54 critically important for HSC efficacy, and may play a role in mitigating the stress response exerted on HSCs  
55 during *in vitro* expansion.

56 Here, we investigated the role of RET at the cell surface of UCB-derived HSCs and the effect of the RET  
57 ligand/co-receptor complex, GDNF/GFR $\alpha$ 1, on outgrowth, initial *in vivo* potency, and long-term stem cell  
58 potential of UCB-derived HSPCs. We monitored key changes in protein signalling cascades, to understand the  
59 intracellular state governed by RET, and provide a mechanism by which activation of RET can be a positive  
60 addition to current culture methods for clinical purposes.

61

## 62 **Methods**

63

### 64 *Primary Human Samples*

65 Umbilical Cord Blood (UCB) was obtained from full term donors after informed consent at the Royal London  
66 Hospital (London, U.K.). Mononuclear cells were isolated by density centrifugation using Ficoll-Paque (GE  
67 Healthcare). Cells were depleted for lineage markers using an EasySep Human Progenitor Cell Enrichment Kit  
68 (Stem Cell Technologies) according to the manufacturer's instructions. Lineage depleted cells were stained with  
69 antibodies listed in the Key Resources Table and sorted using a BD FACS Aria Fusion.

70

### 71 *In Vitro Culture Conditions*

72 Human CD34<sup>+</sup>CD38<sup>-</sup> cells were cultured in StemSpan SFEMII (Stem Cell Technologies) supplemented with  
73 Human SCF (150ng/ml), Human FLT3 ligand (150ng/ml) and Human TPO (20ng/ml; Peprotech) and when  
74 indicated GDNF/GFR $\alpha$ 1 (100ng/ml, GDNF & GFR $\alpha$ 1 mixed 1:1; R&D systems), SR1 (750nM; Stem Cell  
75 Technologies), UM171 (35nM; Stem Cell Technologies), or PZ1 (10nM, Sigma-Aldrich). Cells were incubated  
76 in a tissue culture incubator at 37°C, 5% CO<sub>2</sub> for seven days. For all culture experiments, independent pools of  
77 umbilical cord blood were used for treatments vs control.

78

### 79 *Xenotransplantation Assays*

80 Primary or cultured CD34<sup>+</sup>CD38<sup>-</sup> HSPCs were injected in 8-10 weeks old unconditioned Female NBSGW mice  
81 intravenously (I.V.). Injected mice were euthanised after 12 weeks, in both primary and secondary  
82 transplantations, by cervical dislocation and 6 rear bones and spleen were collected. Bone marrow was flushed  
83 by centrifugation, spleens were crushed and passed through a 100 $\mu$ M strainer, and resulting cells were incubated  
84 in red blood cell lysis buffer (155mM NH<sub>4</sub>Cl, 12mM NaHCO<sub>3</sub>, 0.1mM EDTA) for 5 minutes at room  
85 temperature. Remaining cells were stained with antibodies listed in the Key Resources Table and sorted and  
86 analysed using a BD FACS Aria Fusion. Secondary transplantations were conducted as per primary  
87 transplantations using Human CD45 positive cells sorted from primary mice as donors.

88

89 See further methods description in supplementary information

90

## 91 **Results**

92

### 93 *The receptor tyrosine kinase, RET, is more active in CD34<sup>+</sup>CD38<sup>-</sup> HSPCs than CD34<sup>+</sup>CD38<sup>+</sup> HPCs*

94 In Human UCB, the CD34<sup>+</sup>CD38<sup>-</sup> compartment (HSPCs) contains HSCs able to engraft long-term  
95 in immunodeficient mouse models. In comparison, the CD34<sup>+</sup>CD38<sup>+</sup> compartment (HPCs) contains more

96 differentiated progenitor cells, and has no long-term HSC function in immunodeficient mice. We used PamGene  
 97 kinome array technology to identify kinase activity differences, between the HSPC and HPC compartments  
 98 (Supp. Fig. 1A).

99 Cell extracts from HSPCs and HPCs phosphorylated a range of peptides (Supp. Fig. 1B), and could be clearly  
 100 separated by cell cycle phosphorylations (e.g. RB<sup>pS807/S811</sup>, Supp. Fig. 1C) and classical hematopoietic signalling  
 101 molecules (e.g. AKT1<sup>pY326</sup>, PRKDC<sup>pS2624/S2626</sup>; Supp. Fig. 1D-E). Upstream kinase analysis of the  
 102 phosphorylations by HSPC extracts provides a functional annotation, assigning phosphorylation kinetics to  
 103 kinase activities. This revealed an enrichment for well described kinases such as JAK1/2 and FLT1/3/4 in the  
 104 HSPC compartment (Figure 1A).

105 Differential phosphorylation events (Supp. Fig. 1A) and kinase activities (Figure 1A) between HSPCs and  
 106 HPCs showed strong enrichment in anti-apoptosis signalling, both by PI3K/AKT (FDR = 3.74E-13, 18 proteins)  
 107 and MAPK/JAK/STAT (FDR = 1.896E-11, 15 proteins), erythropoietin signalling (FDR = 1.167E-10, 13  
 108 proteins) and inflammatory pathways including; IL-2 signalling (FDR = 4.045E-07, 9 proteins), TREM1  
 109 signalling (FDR = 4.726E-07, 10 proteins) and IFN-gamma signalling (FDR = 4.726E-07, 9 proteins; Figure  
 110 1B).

111 Interestingly, the receptor tyrosine kinase, RET, was specifically enriched in the HSPC fraction, with a mean  
 112 final score of 2.3 based on 17 peptide phosphorylations (Figure 1A). RET is a transmembrane receptor tyrosine  
 113 kinase, with well-defined ligand/co-receptor interactions, and publicly available datasets indicate that within the  
 114 HSPC compartment, the *RET* gene is expressed at significantly higher levels in HSCs than more differentiated  
 115 progenitor cells (Supp. Fig. 1F). RET signalling, at the cell surface, shows a diverse array of responses in  
 116 different cell types, and considering the well-defined ligand/co-receptor activation interaction<sup>13</sup>, evidence of  
 117 GFL support from the niche<sup>14</sup>, and bio-available stimulating factors *in vitro*<sup>15</sup>, provided an excellent candidate  
 118 for further investigation.

119

#### 120 *RET cell surface expression functionally enriches for stem cell activity in the HSPC compartment*

121 The RET protein must be at the cell surface for ligand/co-receptor-dependent transduction of signals across the  
 122 membrane<sup>16</sup>. When probing for RET at the cell surface, immunophenotypic HSCs (CD34<sup>+</sup>CD38<sup>-</sup>CD45RA<sup>-</sup>  
 123 CD90<sup>+</sup>CD49f<sup>+</sup>) typically show higher RET cell surface expression than MPPs (Multipotent progenitors;  
 124 CD34<sup>+</sup>CD38<sup>-</sup>CD45RA<sup>-</sup>CD90<sup>-</sup>CD49f<sup>-</sup>; Figure 1C & Supp. Fig. 1G-J; gating as per Notta et al. 2011<sup>17</sup>). Multiple  
 125 markers have been proposed to further purify HSCs within the CD34<sup>+</sup>CD38<sup>-</sup> compartment, and we sought to  
 126 investigate the stem/progenitor cell frequency of cells expressing RET at the cell surface after 12 weeks *in*  
 127 *vivo*. Selection of CD34<sup>+</sup>CD38<sup>-</sup> cells solely classified for cell surface expression of RET enriches for HSPC  
 128 stem cell activity in an *in vivo* limiting dilution assay, with high RET HSPCs (RET<sup>hi</sup>) showing a stem cell  
 129 frequency of ~1 in 135 cells and RET<sup>low</sup> HSPCs showing an almost 4-fold reduction in stem cell frequency of  
 130 ~1 in 531 cells (p = 0.026, Figure 1D&E, Supp. Fig. 2A). In addition, RET<sup>hi</sup> HSPCs show much more classical  
 131 lineage balance in immunodeficient mice, whereas RET<sup>low</sup> HSPCs are more myeloid biased (Supp. Fig. 2B).

132

#### 133 *Activation of RET by GDNF/GFR $\alpha$ 1 improves survival and expansion of HSPCs*

134 A key question in hematopoietic stem cell biology remains how to grow HSCs *in vitro* for both engineering and  
 135 expansion purposes<sup>18</sup>. Currently, CD34<sup>+</sup>CD38<sup>-</sup> HSPCs can be grown in culture for 7 days with a minimal

136 cocktail of cytokines, including: SCF, FLT3L and TPO, retaining enough functional HSCs to  
137 engraft immunodeficient mice<sup>19</sup>. To understand the role of RET at the surface of HSPCs and whether this could  
138 be a target for HSC maintenance and expansion, we added its primary ligand/co-receptor combination,  
139 GDNF/GFR $\alpha$ 1 to the culture medium in addition to SCF/FLT3L/TPO and cultured 5,000 HSPCs for 7 days  
140 (Figure 2A). HSPCs expand up to 40-fold in minimal serum free, SCF/FLT3/TPO supplemented conditions  
141 over 7 days. The addition of GDNF/GFR $\alpha$ 1 significantly increased the number of HSPCs by 71-fold at day 7  
142 compared to input cells (Figure 2B).

143 It has previously been reported that EPCR expression marks expanded CD34<sup>+</sup> cord blood stem cells in culture<sup>20</sup>,  
144 and we used this marker in combination with CD90 to estimate the number of expanded HSCs in control and  
145 GDNF/GFR $\alpha$ 1 treated conditions. The frequency of immunophenotypic HSCs within the cultures  
146 (CD34<sup>+</sup>CD90<sup>+</sup>EPCR<sup>+</sup>) was significantly enriched by GDNF/GFR $\alpha$ 1 treatment at both day 3 (Figure 2C) and  
147 day 7 (Figure 2D & Supp. Fig. 3A-C).

148

#### 149 *GDNF/GFR $\alpha$ 1 cultured HSPCs have improved long-term in vivo engraftment*

150 The gold standard for Human HSC functionality under laboratory conditions is engraftment in immunodeficient  
151 mouse models to reveal stem/progenitor (primary engraftment for 12 weeks) and long-term self-renewing HSC  
152 (secondary engraftment for 12 weeks) function. The observed increase in cell numbers in the GDNF/GFR $\alpha$ 1  
153 cultures at day 7 may correlate with outgrowth of functional stem cells in this system, or may be due to another  
154 factor such as increased progenitor cell proliferation<sup>21</sup>. To test the stem cell potency of cultured HSPCs in the  
155 presence of GDNF/GFR $\alpha$ 1, we retrieved all cells from culture replicates at day 7 and transplanted them into  
156 immunodeficient mice harbouring the cKit<sup>W41</sup> mutation (1well:1mouse; NBSGW). Bone marrow and splenic  
157 engraftment was significantly higher after GDNF/GFR $\alpha$ 1 treatment compared to control. The enhanced  
158 engraftment resulting from RET activation was comparable to the previously published combination of  
159 SR1/UM171, and the combination of SR1/UM171/GDNF/GFR $\alpha$ 1 further improved engraftment (Figure 2E,  
160 Supp. Fig. 3D-F). These data indicate that activation of RET can improve progenitor activity for colonising  
161 primary recipients as a single addition to classical SCF/FLT3L/TPO cytokines, similar to that of SR1/UM171.  
162 Analysis of the immunophenotypic HSC compartment within the HuCD45<sup>+</sup> cells from the bone marrow of  
163 primary recipient mice revealed a significant enrichment in all treatment cases (GDNF/GFR $\alpha$ 1, SR1/UM171  
164 and SR1/UM171/GDNF/GFR $\alpha$ 1) compared to controls (Figure 2F). Together, these data indicate improved  
165 expansion of stem/progenitor cells treated with GDNF/GFR $\alpha$ 1, and expansion *in vivo* of phenotypic long-term  
166 HSCs.

167 To test the long-term self-renewal HSC function and frequency of GDNF/GFR $\alpha$ 1 treated cells, we engrafted  
168 HuCD45<sup>+</sup> cells obtained from the bone marrow of primary mice into secondary recipients in a limiting dilution  
169 fashion. Primary cells from GDNF/GFR $\alpha$ 1, SR1/UM171 and SR1/UM171/GDNF/GFR $\alpha$ 1 treatments, engrafted  
170 secondary mice significantly better than controls at the highest dose tested (Figure 2G; Supp. Fig. 3G-I; 2x10<sup>5</sup>  
171 hCD45<sup>+</sup> injected). The estimation of stem cell frequency by ELDA (Extreme Limiting Dilution Analysis)  
172 indicated that control cells have very low long-term stem cell frequency (~1 in 1,500,000). GDNF/GFR $\alpha$ 1  
173 treatment significantly improved long-term stem cell frequency by more than 75-fold (~1 in 20,000). This was  
174 also improved in the SR1/UM171 treated cells (~1 in 41,000), and the combination of

175 SR1/UM171/GDNF/GFR $\alpha$ 1 treatment was similar to GDNF/GFR $\alpha$ 1 treatment alone with a moderate  
 176 improvement ( $\sim$ 1 in 13,000; Figure 2H, Supp. Fig. 3H&J), indicating that GDNF/GFR $\alpha$ 1 provides significant  
 177 improvement in LT-HSC production. Considering initial cell expansion, total engraftment in primary mice,  
 178 percentage of total bone marrow represented by rear leg long bones ( $\sim$ 20%) and long-term stem cell frequency  
 179 in secondary recipients, GDNF/GFR $\alpha$ 1 treatment increases HSC outgrowth over the experimental course  
 180 compared to control conditions by approximately 148-fold ( $\sim$ 742 versus  $\sim$ 5 stem cells produced, respectively),  
 181 compared to SR1/UM171 by approximately 1.3-fold ( $\sim$ 565 stem cells produced) and is further improved by the  
 182 triple combination ( $\sim$ 1,275 stem cells produced, Supp. Fig. 3K).

183

### 184 RET activation induces a dynamic change in the kinome of HSPCs

185 To understand the specific changes governed by RET activation in HSPCs, we investigated functional changes  
 186 in the kinome after GDNF/GFR $\alpha$ 1 treatment using PamGene kinase profiling. We compared functional changes  
 187 in both Serine/Threonine (Figure 3A) and Tyrosine (Figure 3B) kinases in HSPCs at days 0, 1 and 3 post  
 188 GDNF/GFR $\alpha$ 1 treatment. As GDNF/GFR $\alpha$ 1 is rapidly used and turned over *in vitro*, day 1 changes represent  
 189 the acute early events, and day 3 changes represent longer-reaching changes in the kinome of treated HSPCs.

190 At the early time point after GDNF/GFR $\alpha$ 1 treatment (day 1), significant phosphorylations on chip (Figure 3C)  
 191 were predominantly representative of Tyrosine kinase activity (Figure 3D, Supp. Fig. 4A). At the late time point  
 192 after GDNF/GFR $\alpha$ 1 treatment (day 3), significant phosphorylations on chip (Figure 3E) were predominantly  
 193 representative of Serine/Threonine kinase activity (Figure 3F, Supp. Fig. 4B).

194 The early changes at day 1 were enriched in process networks for anti-apoptotic PI3K/AKT signalling ( $p=1.8e-$   
 195  $7$ ), anti-inflammatory IL2 signalling ( $p=1.9e-6$ ), anti-apoptotic MAPK/JAK/STAT signalling ( $p=5.3e-5$ ) and  
 196 Notch signalling ( $p=1.4e-4$ ; Figure 4A). At day 3 changes were enriched for the same process networks seen at  
 197 day 1 (Figure 4A), indicating that fundamental pathways are sustained beyond the immediate GDNF/GFR $\alpha$ 1  
 198 downstream signalling, converging on anti-apoptosis and anti-inflammation.

199 Differential phosphorylation events exclusively at the early time point (day 1; Figure 4B-C) include: cell cycle  
 200 components CDK2<sup>pY15</sup> and RB<sup>pT356</sup> (indicative of an exit from mitosis and progression through the G1/S  
 201 boundary; Figure 4D&E), interleukin signalling components (e.g. JAK3<sup>pY980/981</sup>, Supp. Fig. 5B) and the p53  
 202 anti-apoptotic phosphorylations at p53<sup>pT18</sup> and p53<sup>pS315</sup> (Figure 4F&G). These phosphorylation events indicate  
 203 that cells treated with GDNF/GFR $\alpha$ 1 at early time points are more positively cycling, have an earlier anti-  
 204 inflammatory response and increased anti-apoptotic activity.

205 In normoxic cultures, anti-inflammatory and anti-apoptotic signalling are important for HSC maintenance,  
 206 expansion and survival, and phosphorylation networks in day 3 GDNF/GFR $\alpha$ 1 treated cells represent a  
 207 convergence on these key pathways (Figure 4J). For example, the phosphorylation of BAD<sup>pS99</sup>, which is hyper-  
 208 phosphorylated when cells are under stress and are resisting apoptosis<sup>22</sup>, is reduced under GDNF/GFR $\alpha$ 1  
 209 treatment (Figure 4K). Upstream, FOXO3, the transcription factor responsible for expression of another pro-  
 210 apoptotic factor, *BIM*, also shows reduced phosphorylation at S30/T32 in GDNF/GFR $\alpha$ 1 treated cells,  
 211 indicating there is a block in expression of pro-apoptotic genes such as *BIM* (Figure 4L). In addition, RB  
 212 phosphorylation switches, and there is a significant reduction in RB<sup>pS807/811</sup>, resulting in less potential for BAX  
 213 binding and further indication that anti-apoptotic functions are no longer required (Figure 4M). This switch in  
 214 phosphorylation events between early and late time points coincides with the emergence of kinase activity by



215 IKK complex members (IKK $\alpha$ , IKK $\beta$  and IKK $\epsilon$ ; Figure 3F & Supp. Fig. 4B), a pathway known to  
216 be downstream of RET induced AKT/ERK activity<sup>23</sup>. These pathways indicate that a mechanism of protection  
217 by GDNF/GFR $\alpha$ 1 treatment at later time points is due to protection against apoptosis through RET-induced  
218 AKT/ERK activity and downstream via NF $\kappa$ B signalling.

219 Next, we sought to understand how GDNF/GFR $\alpha$ 1 treatment mitigates changes from input cells over time  
220 compared to controls. Whilst there is clear concordance between phosphorylation changes from input cells to  
221 day 1 controls and GDNF/GFR $\alpha$ 1 treatment ( $R = 0.56$ ,  $p < 2.2e-16$ ; Supp. Fig. 4C), and from input cells to day  
222 3 controls and GDNF/GFR $\alpha$ 1 treatment ( $R = 0.75$ ,  $p < 2.2e-16$ ; Supp. Fig. 4D), there are key peptide changes  
223 seen exclusively in control cells or in GDNF/GFR $\alpha$ 1 treated cells at each time point (Supp. Fig. 4E). The most  
224 highly changed phosphorylation site in day 1 control cultures compared to input cells is, DSP<sup>pS2849</sup>, which  
225 remains unchanged throughout all other conditions (Supp. Fig. 5A). The DSP<sup>pS2849</sup> phospho-site is dependent on  
226 GSK3 $\beta$  and PKACA activity, which are important kinases involved in normal and malignant hematopoiesis, and  
227 phosphorylation at this site reduces desmoplakin-mediated adhesion to extracellular matrices (Supp. Fig. 5A)<sup>24</sup>.  
228 At day 3, control cells uniquely lack: ADDB<sup>pS697/S701</sup>, phospho-sites associated with induction of cell growth,  
229 notably a site that is better maintained throughout by GDNF/GFR $\alpha$ 1 supplementation (Supp. Fig. 5D).

230 Conversely, at day 1 culture with GDNF/GFR $\alpha$ 1, the p53<sup>pS315</sup> phospho-site is significantly increased (Figure  
231 4G), a site known to be phosphorylated by CDK1 and important for anti-apoptotic functions. In addition to  
232 improved survival phosphorylation events at day 1, by day 3, GDNF/GFR $\alpha$ 1 treated cultures also display major  
233 reductions when compared to controls in phosphorylation of IF4E<sup>pS209/T210</sup> (Supp. Fig. 5E) and RB<sup>pS807/S811</sup>,  
234 indicative of cell cycle alterations and anti-apoptotic functions (Figure 4M).

235 These profiles indicate that overlapping and independent phosphorylation changes between control and  
236 GDNF/GFR $\alpha$ 1 treated cultures lead to diverse pathway activation. These signalling alterations are likely to be  
237 responsible for the differences in functional output of HSPCs.

238

### 239 *GDNF/GFR $\alpha$ 1 treatment sustains an integrated cell survival and proliferation program in cultured HSPCs*

240 Despite the wide-scale dynamic changes in the kinome, key regulatory phosphorylation cascades surrounding an  
241 NF $\kappa$ B/p53/BCL2 cell survival and proliferation program were consistently affected at early and late time points.  
242 We sought to utilise mass cytometry to investigate the dynamics of these phosphorylation steps and protein  
243 abundance in CD34<sup>+</sup> cells after initial isolation, at early (day 3) and late (day 7) expansion time points (Figure  
244 5A&B). RET is hyper-phosphorylated after GDNF/GFR $\alpha$ 1 treatment at day 3 compared to controls and reduces  
245 over time as GDNF/GFR $\alpha$ 1 depletion occurs. In contrast, total RET abundance increased early and continued to  
246 increase at day 7 (Figure 5A&B).

247 Many of the key factors identified throughout our kinome analysis are downstream of RET, mediated by one of  
248 two key signalling cascade partners, AKT and ERK. Interestingly, both AKT<sup>pS473</sup> and ERK1/2<sup>pT202/Y204</sup> mirror  
249 RET phosphorylation, and are activated early. ERK phosphorylation was sustained over time, whereas AKT  
250 increased further at day 7 (Figure 5A&B).

251 Downstream of AKT/ERK activity, we observed increased p53<sup>pS392</sup>, which induces interaction with NF $\kappa$ B, and  
252 in addition we observed increased NF $\kappa$ B transcriptional activity (Figure 5A-C & Supp. Fig. 6A&B). This

253 NFκB/p53 axis is an important regulator of the cell survival and growth characteristics we observed in our *in*  
254 *vitro* cultures.

255 When assessing the downstream genetic targets of these key proteins, we observed significant down-regulation  
256 of the FOXO3, pro-apoptotic target, *BIM*, and significant up-regulation of anti-apoptotic NFκB target genes  
257 *BCL2* and *TP53*, but not consistent changes in NFκB pro-inflammatory target genes *TNF-alpha* and *IL1-beta*  
258 (Figure 5C, Supp. Fig. 6A&B). To further confirm that the changes we see are caused acutely by  
259 phosphorylation cascades downstream of GDNF/GFRα1 treatment, and not secondary to transcriptomic  
260 adaptations, we monitored RNA levels of key components of this pathway, altered at the protein level, including;  
261 *FOXO3A*, *RELA*, *ELK1* and *IKBKB* (Figure 5D). Indeed, *FOXO3A*, *ELK1* and *IKBKB* remain similar to controls  
262 until the late time point (day 7), at which, *FOXO3A* and *IKBKB* are upregulated (*ELK1* remained constant  
263 throughout), presumably as feedback in response to their inactivity at the protein level. In contrast, *RELA* is  
264 initially downregulated early (day 1) and increases over time. Therefore, activation of RET induced changes at  
265 the protein phosphorylation and total abundance levels are the predominant effectors of the response observed,  
266 with input from transcriptional changes contributing a smaller part of the downstream effectors mediating the  
267 phenotypic response.

268 These data provide a two-pronged mechanism, by which RET activation induces the activity of AKT and ERK  
269 as key signalling hubs to drive a cell survival and proliferation program in HSPCs *in vitro*. The  
270 NFκB/p53/BCL2 axis provides a stable platform for HSPCs to survive and expand in culture before  
271 transplantation *in vivo* (Figure 5E).

272

### 273 HSCs have a specific response mechanism to GDNF/GFRα1 in culture

274 Protein changes responsive to GDNF/GFRα1 treatment, monitored in CD34<sup>+</sup> cells during culture, were  
275 consistent within the immunophenotypic HSC compartment of cultured cells (CD34<sup>+</sup>CD38<sup>-</sup>CD45RA<sup>-</sup>CD90<sup>+</sup>),  
276 but less responsive in the MPP compartment (CD34<sup>+</sup>CD38<sup>-</sup>CD45RA<sup>-</sup>CD90<sup>-</sup>), indicating a specific response  
277 mechanism in HSCs (Supp. Fig. 7A&B). In addition, at day 0 HSCs have higher total RET than MPPs (but not  
278 bulk CD34<sup>+</sup>CD38<sup>-</sup>), and HSCs show the strongest RET<sup>Y905</sup> signal of all compartments (data not shown),  
279 indicating that RET signalling is already primed in HSCs pre-culture.

280 In comparison to control cultures, HSCs show a strong response at day 3 to GDNF/GFRα1 by increases in  
281 RET<sup>Y905</sup>, AKT<sup>S473</sup> and ERK1/2<sup>T202/Y204</sup> (Figure 6A&B). In addition, NFκB<sup>S529</sup> and p53<sup>S392</sup> are upregulated at  
282 day 3 by GDNF/GFRα1 treatment, indicating the cell survival and oxidative stress response network discovered  
283 in bulk HSPCs (Figure 5A&B) is similarly stimulated in HSCs (Figure 6A&B). Interestingly, GDNF/GFRα1  
284 treatment also suppresses the abundance of the differentiation pioneer factor, PU.1, at later stages (day 7) whilst  
285 inducing GATA1 expression at early stages (day 3; Figure 6A&B). The changes induced at day 3 by  
286 GDNF/GFRα1, are generally spikes in signalling, lost upon the exhaustion of ligand/co-receptor. Only 4  
287 proteins remain more abundant in GDNF/GFRα1 treated culture (STAT5<sup>Y694</sup>, ERK1/2<sup>T202/Y204</sup>, S6<sup>S235/S236</sup>,  
288 cREL and Ki67), indicating that the spike in activity early is enough to induce a survival and expansion program  
289 in HSCs in culture (Figure 6A&B, Supp. Fig. 7A&B).

290 In agreement with our earlier findings of anti-apoptotic and anti-inflammatory signatures (Figure 4A), HSCs  
291 show a specific spike in p53<sup>S392</sup> at day 3, but no upregulation of NFκB<sup>S529</sup> (Figure 6A&B). *In vitro* this leads to  
292 a reduction in intracellular reactive oxygen species (ROS) for both bulk CD34<sup>+</sup> cells, and specifically HSCs

293 (Figure 6C&D, Supp. Fig. 8 C&D). When inhibiting RET signalling, with the pan-RET/VEGFR2 inhibitor PZ1  
294 (Supp. Fig. 8A), the reduction in intracellular ROS is abolished, and the number of CD34<sup>+</sup> cells, and more  
295 importantly HSCs, in culture is lost (Figure 6E, Supp. Fig. 8E), with CD34<sup>+</sup> cells showing a significant increase  
296 in apoptosis in response to PZ1 at day 7 (Supp. Fig. 8B). Together, these data indicate that the tailored response  
297 in HSCs is critically dependent on RET signalling maintaining fundamental stress response pathways during *in*  
298 *vitro* outgrowth.

299

## 300 **Discussion**

301

302 The use of UCB for hematopoietic stem cell transplantation is a rapidly increasing treatment option for both  
303 hematological and non-hematological malignancies, as well as new gene therapy and regenerative medicine  
304 approaches. The current outcomes from cord blood transplantation are limited primarily by low stem cell dose  
305 and delayed hematopoietic recovery<sup>4</sup>. Early strategies to grow HSCs *in vitro* induce a large amount of  
306 differentiation in culture<sup>19</sup>, but recent improvements in expansion of HSCs, such as those conferred by SR1,  
307 UM171<sup>25,26</sup> and here, GDNF/GFR $\alpha$ 1, *in vitro*, provide a positive platform for improvement of UCB-derived  
308 HSCs *in vivo*.

309 Our finding of higher RET activity in HSPCs derived from UCB may be due to cell-intrinsic mechanisms/  
310 autocrine signalling loops or from specific niche components. Indeed, there is evidence of enervation of the  
311 HSC bone marrow niche, and recent high dimensional analysis of niche components reveal expression of GFLs  
312 from COL2.3<sup>+</sup> osteoblasts<sup>14</sup>. Therefore, the provision of GDNF/GFR $\alpha$ 1 may be a key component, already  
313 provided by the bone marrow niche, for HSCs to maintain their potential *in vitro*. Regardless of the source of  
314 activation, the increased phosphorylation of RET in phenotypic HSCs from UCB indicates an active RET  
315 signalling pathway *in vivo*, specifically tailored to HSCs.

316 We provide a mechanism by which RET can govern an anti-apoptotic and anti-inflammatory program, due to  
317 diverging and exclusive contributions to the same goal, to improve survival and expansion of HSCs for  
318 regenerative and engineering purposes. A key issue when expanding HSCs *in vitro* is the need to grow them in  
319 normoxic conditions for maximum expansion. The induction of oxidative stress under these conditions can lead  
320 to a loss in stem cell activity<sup>27,28</sup>. The stimulation of RET signalling can reduce the accumulation of ROS in  
321 HSCs and maintain their potency, whilst providing further signals to expand *in vitro*. Interestingly, the basic  
322 complement of cytokines used to grow HSPCs in culture (SCF/FLT3L/TPO) is known to activate ERK/AKT  
323 signalling<sup>29</sup>. Our findings that this is strongly enhanced by the activation of RET indicates that there is both  
324 capacity to increase these signalling cascades (strength and time of response), and improve the diversity of the  
325 response (in our case the I $\kappa$ B $\alpha$  arm, Figure 5E), ultimately leading to improvement in HSC function over the  
326 experimental course. The addition of UM171 to SCF/FLT3L/TPO when culturing HSPCs has also been shown  
327 to re-tune NF $\kappa$ B pro- and anti-inflammatory activity, through EPCR, ultimately reducing the ROS burden in  
328 HSCs *in vitro*<sup>30</sup>. Although it is unknown what the direct target of UM171 is, it is possible that association with  
329 EPCR function may activate AKT/ERK signalling and even stimulate RET activity to some extent. Yet, the  
330 reduction of estimated stem cells produced by SR1/UM171 compared to GDNF/GFR $\alpha$ 1 (Supp. Fig. 3H)

331 indicates that classical stimulation of RET activity (by GFLs) has a stronger effect than UM171 if this is the  
332 case.

333 In addition to potential improvements in patient outcome, improved outgrowth of UCB-derived HSCs can begin  
334 to address the issue of double cord blood transplantation and associated costs, increasing the practicality of  
335 using UCB banks in frontline treatment<sup>4</sup>. These benefits could potentially provide an immediate improvement to  
336 clinical outcomes, but also, with the rapidly increasing promise of gene therapy, improvements in survival  
337 during expansion may provide a critical edge to genetic engineering protocols for future therapies.

338

### 339 **Acknowledgements**

340 We would like to acknowledge the Francis Crick Core flow cytometry and biological research facility STPs.  
341 D.B acknowledges that this work was supported by the Francis Crick Institute, which receives its core funding  
342 from Cancer Research UK (FC001115), the UK Medical Research Council (FC001115) and the Wellcome Trust  
343 (FC001115); N.Q.M research was also partly funded by the Francis Crick and by the NCI/NIH (grant reference  
344 5R01CA197178) and by the Association for Multiple Endocrine Neoplasia Disorders MTC Research Fund. We  
345 would also like to thank Dr. Constandina Pospori for critical feedback on the manuscript.

346

### 347 **Author contributions**

348 W.G. designed and carried out experiments, analysed the data and wrote the manuscript. R.C., M.P., H.H.E &  
349 M.G-A. carried out experiments. N.Q.M. supervised the project. D.B. supervised the project and wrote the  
350 manuscript. All authors provided critical feedback on the manuscript.

351

### 352 **Conflict of Interest**

353 The authors declare no relevant conflicts of interest.

354

### 355 **References**

- 356 1. Broxmeyer HE. Enhancing the efficacy of engraftment of cord blood for hematopoietic cell  
357 transplantation. *Transfus. Apher. Sci.* 2016;
- 358 2. Miller PH, Knapp DJHF, Eaves CJ. Heterogeneity in hematopoietic stem cell populations. *Curr. Opin.*  
359 *Hematol.* 2013;20(4):257–264.
- 360 3. Brunstein CG, Gutman JA, Weisdorf DJ, et al. Allogeneic hematopoietic cell transplantation for  
361 hematologic malignancy: relative risks and benefits of double umbilical cord blood. *Blood.*  
362 2010;116(22):4693–9.
- 363 4. Ballen KK, Joffe S, Brazauskas R, et al. Hospital Length of Stay in the First 100 Days after Allogeneic  
364 Hematopoietic Cell Transplantation for Acute Leukemia in Remission: Comparison among Alternative  
365 Graft Sources. *Biol. Blood Marrow Transplant.* 2014;20(11):1819–1827.
- 366 5. Boitano AE, Wang J, Romeo R, et al. Aryl Hydrocarbon Receptor Antagonists Promote the Expansion  
367 of Human Hematopoietic Stem Cells. *Science (80-. ).* 2010;329(5997):1345–1348.
- 368 6. North TE, Goessling W, Walkley CR, et al. Prostaglandin E2 regulates vertebrate haematopoietic stem  
369 cell homeostasis. *Nature.* 2007;447(7147):1007–1011.

- 370 7. Goessling W, Allen RS, Guan X, et al. Prostaglandin E2 Enhances Human Cord Blood Stem Cell  
371 Xenotransplants and Shows Long-Term Safety in Preclinical Nonhuman Primate Transplant Models.  
372 *Cell Stem Cell*. 2011;8(4):445–458.
- 373 8. Hoggatt J, Singh P, Sampath J, Pelus LM. Prostaglandin E2 enhances hematopoietic stem cell homing,  
374 survival, and proliferation. *Blood*. 2009;113(22):5444–5455.
- 375 9. Xie SZ, Garcia-Prat L, Voisin V, et al. Sphingolipid Modulation Activates Proteostasis Programs to  
376 Govern Human Hematopoietic Stem Cell Self-Renewal. *Cell Stem Cell*. 2019;0(0):
- 377 10. Guo B, Huang X, Lee MR, Lee SA, Broxmeyer HE. Antagonism of PPAR- $\gamma$  3 signaling expands human  
378 hematopoietic stem and progenitor cells by enhancing glycolysis. *Nat. Med*. 2018;
- 379 11. Huang X, Guo B, Capitano M, Broxmeyer HE. Past, present, and future efforts to enhance the efficacy  
380 of cord blood hematopoietic cell transplantation [version 1; peer review: 3 approved]. *F1000Research*.  
381 2019;
- 382 12. Fonseca-Pereira D, Arroiz-Madeira S, Rodrigues-Campos M, et al. The neurotrophic factor receptor  
383 RET drives haematopoietic stem cell survival and function. *Nature*. 2014;514(7520):98–101.
- 384 13. Mulligan LM. RET revisited: Expanding the oncogenic portfolio. *Nat. Rev. Cancer*. 2014;
- 385 14. Tikhonova AN, Dolgalev I, Hu H, et al. The bone marrow microenvironment at single-cell resolution.  
386 *Nature*. 2019;569(7755):222–228.
- 387 15. Richardson DS, Lai AZ, Mulligan LM. RET ligand-induced internalization and its consequences for  
388 downstream signaling. *Oncogene*. 2006;25(22):3206–11.
- 389 16. Jing S, Wen D, Yu Y, et al. GDNF-induced activation of the ret protein tyrosine kinase is mediated by  
390 GDNFR-alpha, a novel receptor for GDNF. *Cell*. 1996;85:1113–1124.
- 391 17. Notta F, Doulatov S, Laurenti E, et al. Isolation of single human hematopoietic stem cells capable of  
392 long-term multilineage engraftment. *Science (80-. )*. 2011;
- 393 18. Tajer P, Pike-Overzet K, Arias S, Havenga M, Staal FJT. Ex Vivo Expansion of Hematopoietic Stem  
394 Cells for Therapeutic Purposes: Lessons from Development and the Niche. *Cells*. 2019;8(2):.
- 395 19. Murray LJ, Young JC, Osborne LJ, et al. Thrombopoietin, flt3, and kit ligands together suppress  
396 apoptosis of human mobilized CD34+ cells and recruit primitive CD34+Thy-1+ cells into rapid  
397 division. *Exp. Hematol*. 1999;
- 398 20. Fares I, Chagraoui J, Lehnertz B, et al. EPCR expression marks UM171-expanded CD34+ cord blood  
399 stem cells. *Blood*. 2017;129(25):3344–3351.
- 400 21. Bai T, Li J, Sinclair A, et al. Expansion of primitive human hematopoietic stem cells by culture in a  
401 zwitterionic hydrogel. *Nat. Med*. 2019;25(10):1566–1575.
- 402 22. Moody SE, Schinzel AC, Singh S, et al. PRKACA mediates resistance to HER2-targeted therapy in  
403 breast cancer cells and restores anti-apoptotic signaling. *Oncogene*. 2014;
- 404 23. Gallel P, Pallares J, Dolcet X, et al. Nuclear factor- $\kappa$ B activation is associated with somatic and germ  
405 line RET mutations in medullary thyroid carcinoma. *Hum. Pathol*. 2008;39(7):994–1001.
- 406 24. Stappenbeck TS, Lamb JA, Corcoran CM, Green KJ. Phosphorylation of the desmoplakin COOH  
407 terminus negatively regulates its interaction with keratin intermediate filament networks. *J. Biol. Chem*.  
408 1994;269(47):29351–4.
- 409 25. Fares I, Chagraoui J, Gareau Y, et al. Cord blood expansion. Pyrimidoindole derivatives are agonists of

- 410 human hematopoietic stem cell self-renewal. *Science*. 2014;345(6203):1509–12.
- 411 26. Cohen S, Roy J, Lachance S, et al. Hematopoietic stem cell transplantation using single UM171-  
 412 expanded cord blood: a single-arm, phase 1–2 safety and feasibility study. *Lancet Haematol*. 2020;
- 413 27. Jang YY, Sharkis SJ. A low level of reactive oxygen species selects for primitive hematopoietic stem  
 414 cells that may reside in the low-oxygenic niche. *Blood*. 2007;
- 415 28. Ludin A, Gur-Cohen S, Golan K, et al. Reactive oxygen species regulate hematopoietic stem cell self-  
 416 renewal, migration and development, as well as their bone marrow microenvironment. *Antioxidants*  
 417 *Redox Signal*. 2014;
- 418 29. Knapp DJHF, Hammond CA, Aghaeepour N, et al. Distinct signaling programs control human  
 419 hematopoietic stem cell survival and proliferation. *Blood*. 2017;129(3):307–318.
- 420 30. Chagraoui J, Lehnertz B, Girard S, et al. UM171 induces a homeostatic inflammatory-detoxification  
 421 response supporting human HSC self-renewal. *PLoS One*. 2019;
- 422

### 423 **Figure Legends**

424

425 **Figure 1. RET is functionally active in CD34<sup>+</sup>CD38<sup>-</sup> HSPCs and cell surface expression enriches for HSC**  
 426 **function. A.** Kinase activity alterations between CD34<sup>+</sup>CD38<sup>-</sup> HSPCs (green) and CD34<sup>+</sup>CD38<sup>+</sup> HPCs (lilac).  
 427 **B.** Process network enrichment for significantly altered kinases and phosphorylation events from **A.** **C.** *z*-  
 428 normalized geometric mean fluorescence intensity of cell surface RET within the indicated populations.  
 429 Significance was tested using a paired Student's *t*-test for individual cord blood donors tested (N=9). **D.** Plot  
 430 depicting frequencies and confidence interval for RET<sup>hi</sup>(red) and RET<sup>low</sup>(grey) CD34<sup>+</sup>CD38<sup>-</sup> cell *in vivo*  
 431 engraftment at limiting dilution after 12 weeks (N=3 mice per dose tested). **E.** Table of 1/stem cell frequency  
 432 numerical data calculated from the *in vivo* LDA presented in **D**, including: estimated stem cell frequency, upper  
 433 and lower intervals of estimation, Chi-squared test and estimated p-value.

434

435 **Figure 2. GDNF/GFRα1 treatment stimulates growth of transplantable HSCs. A.** Experimental design for  
 436 GDNF/GFRα1 supplemented outgrowth of HSCs and transplantation ability. 1<sup>o</sup>TP and 2<sup>o</sup>TP represents the first  
 437 and second transplantation respectively. **B.** Live cell count of *in vitro* cultured HSPCs (N=5). Proportion of  
 438 expanded HSCs (CD34<sup>+</sup>CD90<sup>+</sup>EPCR<sup>+</sup>) at day 3 (**C**) and day 7 (**D**) during *in vitro* culture (N=5). **E.** Percentage  
 439 of Human CD45 positive cells of total CD45 positive bone marrow cells in primary transplantation mice (Ctrl  
 440 N=12, GDNF/GFRα1 N=10, SR1/UM171 N=7, SR1/UM171/GDNF/GFRα1 N=6). **F.** Percentage of  
 441 immunophenotypic HSCs (CD34<sup>+</sup>CD38<sup>-</sup>CD45RA<sup>-</sup>CD90<sup>+</sup>CD49f<sup>+</sup>) retained in Human CD45 bone marrow cells  
 442 in primary transplantation mice. **G.** Percentage of Human CD45 positive cells of total CD45 positive bone  
 443 marrow cells in secondary transplantation mice (2x10<sup>5</sup> hCD45 cells transplanted shown, N=5 for all conditions).  
 444 **H.** Boxplot indicating 1/Stem Cell Frequency of secondary transplanted Human CD45 positive cells. Estimates  
 445 with upper and lower intervals are shown (N=5 for top dose, N=3 for all other doses). For all graphs, A  
 446 Student's *t*-test was used to calculated significant differences (\* = p < 0.05 vs Ctrl, \*\* = p < 0.005 vs Ctrl).

447

448 **Figure 3. Activation of RET by GDNF/GFRα1 alters kinome dynamics during HSPC outgrowth.**  
 449 Heatmaps depicting **A.** Serine/Threonine and **B.** Tyrosine containing row *z*-normalized peptide

450 phosphorylations supervised by day and treatment. Rows are clustered by correlation. **C.** Fold change  
451 differential phosphorylation of GDNF/GFR $\alpha$ 1 treated CD34<sup>+</sup>CD38<sup>-</sup> cells compared to control after 1 day of  
452 culture. **D.** Upstream kinases calculated as responsible for phosphorylations in **C.** **E.** Fold change differential  
453 phosphorylation of GDNF/GFR $\alpha$ 1 treated CD34<sup>+</sup>CD38<sup>-</sup> cells compared to control after 3 days of culture. **F.**  
454 Upstream kinases calculated as responsible for phosphorylations in **G.** **C-F:** Red dots indicate significantly  
455 upregulated peptides or kinases, Blue dots represent significantly downregulated peptides or kinases in response  
456 to GDNF/GFR $\alpha$ 1 treatment.

457  
458

459 **Figure 4. GDNF/GFR $\alpha$ 1 treatment induces anti-apoptotic and anti-inflammatory processes in cultured**  
460 **HSPCs.** **A.** Enriched process networks from significantly changed peptides in GDNF/GFR $\alpha$ 1 versus control  
461 cultures after 1 day (left, light red) or 3 days (right, dark red). **B.** Venn diagram depicting overlap of  
462 significantly altered peptides between day 1 (light red) and day 3 (dark red) from GDNF/GFR $\alpha$ 1 versus control  
463 cultures. **C.** String protein network for differential phosphorylation events at day 1. Lines indicate reported  
464 interactions. **D-I.** Key differential phosphorylations induced by GDNF/GFR $\alpha$ 1 treatment at day 1, represented  
465 as relative phosphorylation. A Student's *t*-test was used to measure significant differences. Day 0 CD34<sup>+</sup>CD38<sup>-</sup>  
466 input cells (white), control (black) and GDNF/GFR $\alpha$ 1 (red) treatments at days 1 and 3 are presented. **J.** String  
467 protein network for differential phosphorylation events at day 3. Lines indicate reported interactions. **K-M.** Key  
468 differential phosphorylations induced by GDNF/GFR $\alpha$ 1 treatment at day 3, represented as relative  
469 phosphorylation. A Student's *t*-test was used to measure significant differences. Day 0 CD34<sup>+</sup>CD38<sup>-</sup> input cells  
470 (white), control (black) and GDNF/GFR $\alpha$ 1 (red) treatments at days 1 and 3 are presented.

471

472 **Figure 5. RET activation by GDNF/GFR $\alpha$ 1 sustains an NF $\kappa$ B/p53/BCL2 anti-apoptotic program in**  
473 **HSPCs during *in vitro* culture.** **A.** Bar graphs depict median intensity of signal from histograms below  
474 showing the profiles of key protein changes in CD34<sup>+</sup> cells at day 0 (blue), day 3 control (orange) day 3  
475 GDNF/GFR $\alpha$ 1 (green), day 7 control (red) and day 7 GDNF/GFR $\alpha$ 1 (purple, a.u. = arbitrary units). **B** z-  
476 normalized heatmap of data in **A**, illustrating differences in CD34<sup>+</sup>CD38<sup>-</sup> cells at input, and CD34<sup>+</sup> cells at day 3  
477 and day 7 culture with or without GDNF/GFR $\alpha$ 1 treatment assayed by mass cytometry, supervised by treatment  
478 condition. **C.** Fold change RNA expression of key NF $\kappa$ B target genes in GDNF/GFR $\alpha$ 1 treated CD34<sup>+</sup>CD38<sup>-</sup>  
479 cells compared to controls at days 1, 3 and 7. Gene names are noted under bar labels. A Student's *t*-test was  
480 used to calculate significant differences (\* =  $p < 0.05$ , \*\* =  $p < 0.005$ , N=3 per condition and day tested). **D.**  
481 Fold change RNA expression of key genes altered at the protein level in GDNF/GFR $\alpha$ 1 treated CD34<sup>+</sup>CD38<sup>-</sup>  
482 cells compared to controls at days 1, 3 and 7. Gene names are noted under bar labels. A Student's *t*-test was  
483 used to calculate significant differences (\* =  $p < 0.05$ , \*\* =  $p < 0.005$ , N=3 per condition and day tested). **E.**  
484 Illustrated pathway identified through kinome, mass cytometry and RNA changes, defining activating (green)  
485 and inhibiting (red) phosphorylations, protein levels or RNA levels and proposed modes of action.

486

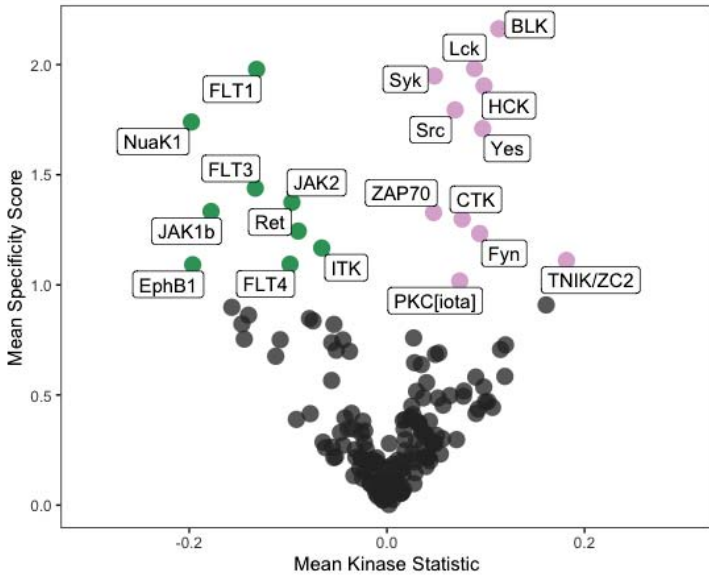
487 **Figure 6. HSCs exhibit specific responses to GDNF/GFR $\alpha$ 1 resulting in reduced accumulation of**  
488 **intracellular ROS.** **A.** Bar graphs depict median intensity of signal from histograms below illustrating profiles

489 of key protein changes in HSCs at day 0 (blue), day 3 control (orange) day 3 GDNF/GFR $\alpha$ 1 (green), day 7  
490 control (red) and day 7 GDNF/GFR $\alpha$ 1 (purple, a.u. = arbitrary units). **B** z-normalized heatmap illustrating  
491 differences in HSC clusters at input, day 3 and day 7 culture with or without GDNF/GFR $\alpha$ 1 treatment assayed  
492 by mass cytometry, supervised by treatment condition. **C**. Mean fluorescence intensity of intracellular ROS in  
493 HSCs at day 7 $\pm$  GDNF/GFR $\alpha$ 1/PZ1 (\* =  $p < 0.05$ , N=4). **D**. Histograms illustrating changes in intracellular  
494 ROS at day 7. **E**. Percentage of HSCs in cultured cells at day 7 $\pm$  GDNF/GFR $\alpha$ 1/PZ1 (\* =  $p < 0.05$ , N=4).

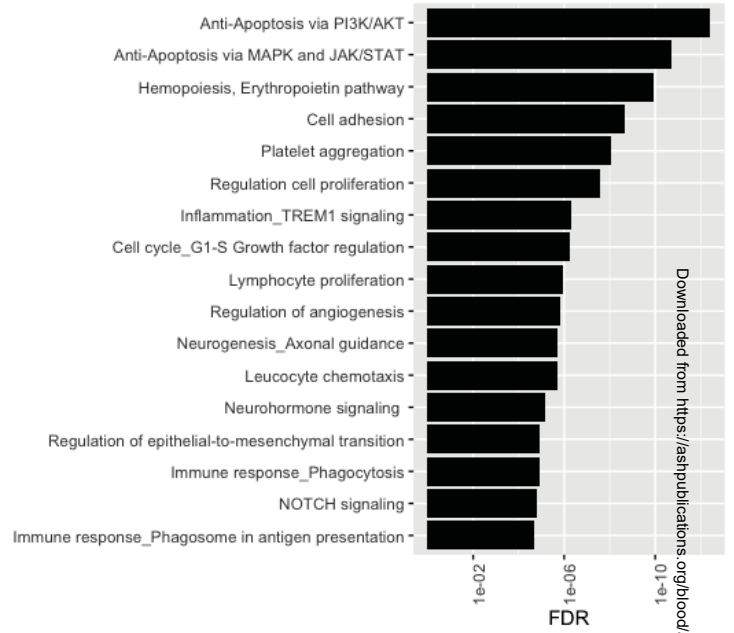


# Figure 1

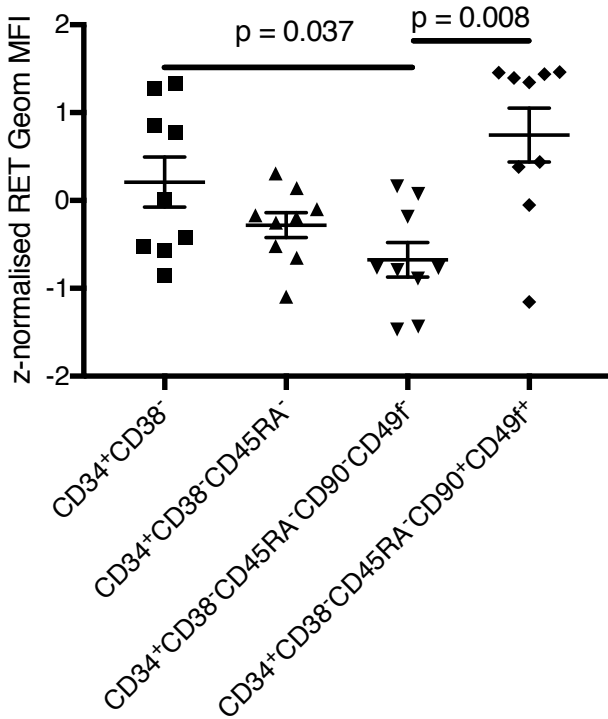
**A**



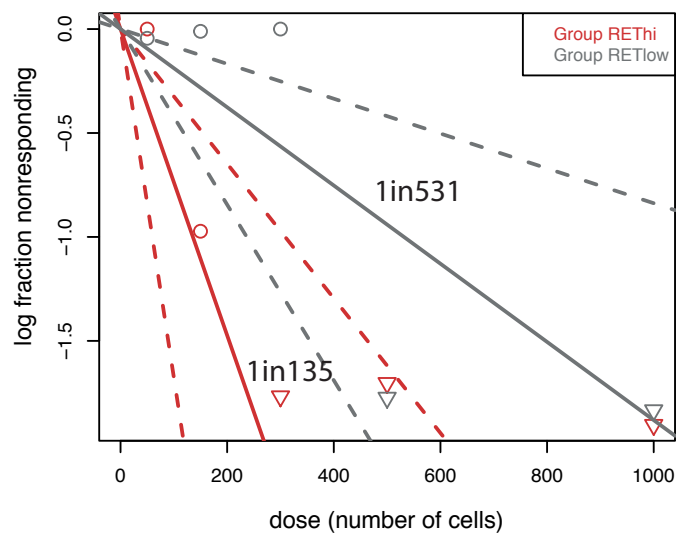
**B**



**C**



**D**



**E**

	Lower	Estimate	Upper
RET <sup>Hi</sup>	308	135	59
RET <sup>Low</sup>	1193	531	236

Chisq 4.93194 on 1 DF  
p-value: 0.02636

# Figure 2

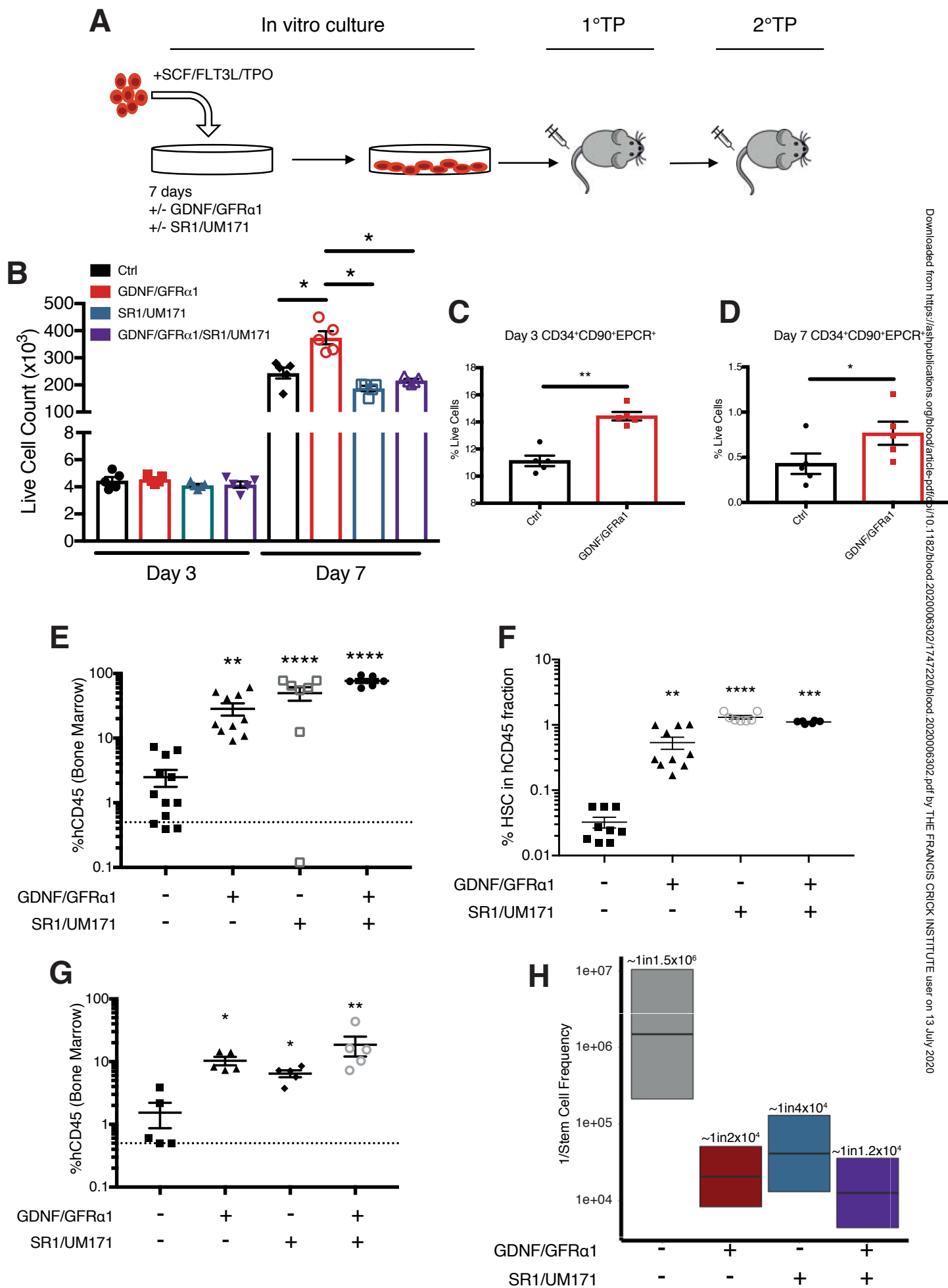
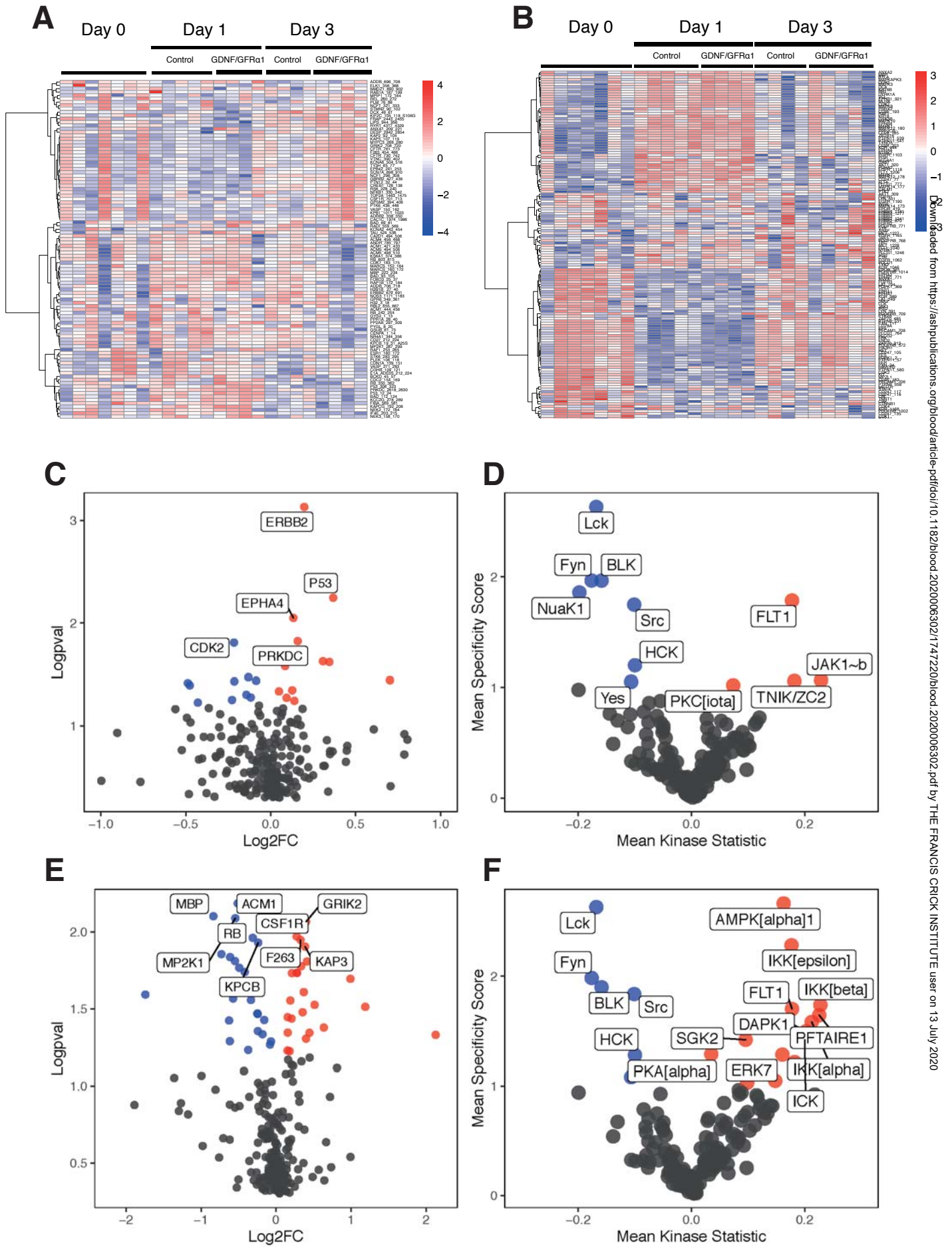


**Figure 3**



Downloaded from https://ashpublications.org/blood/article-pdf/doi/10.1182/blood.2020063027.174720/blood.2020063027.pdf by THE FRANCIS CRICK INSTITUTE user on 13 July 2020

# Figure 4

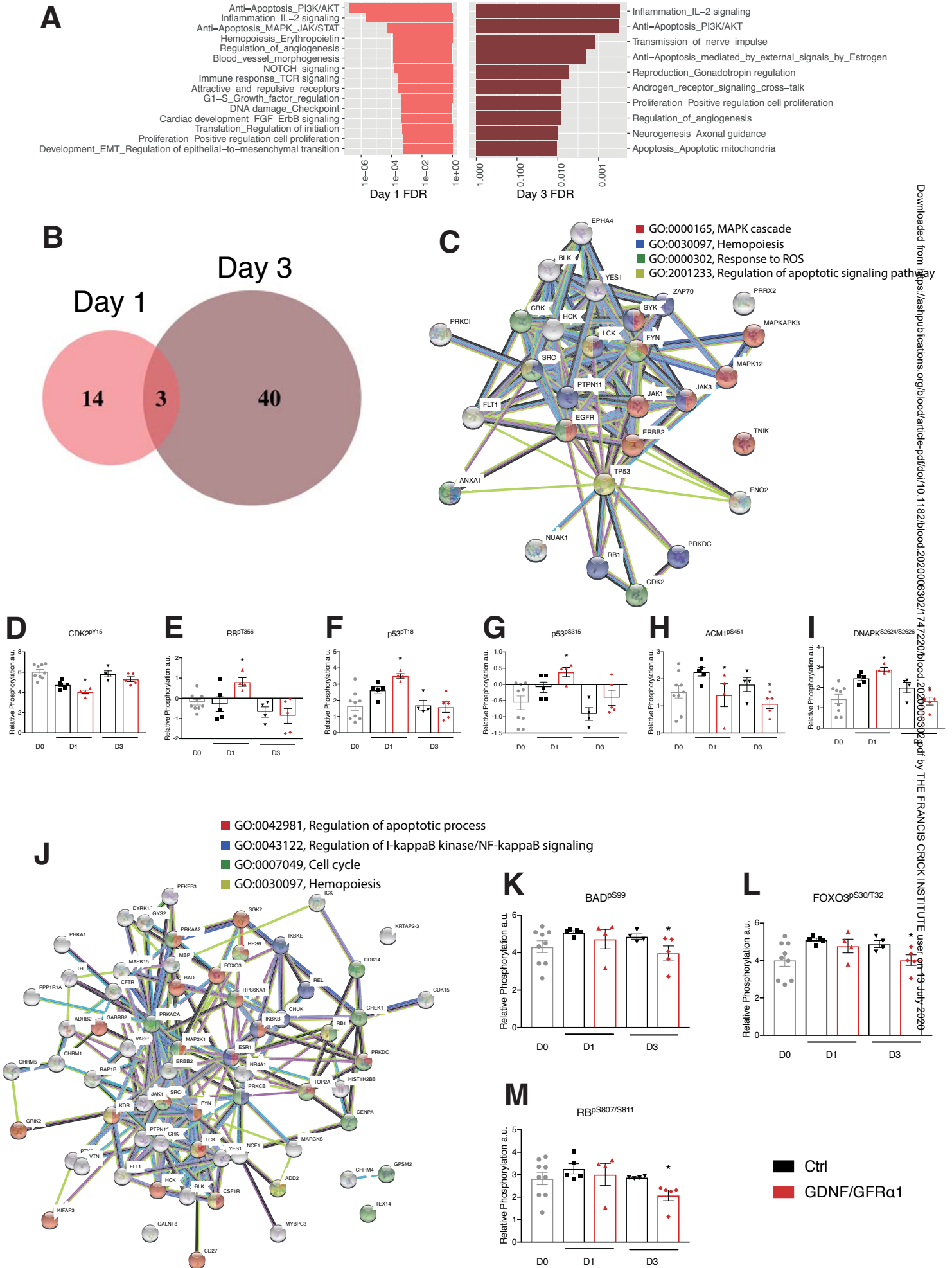
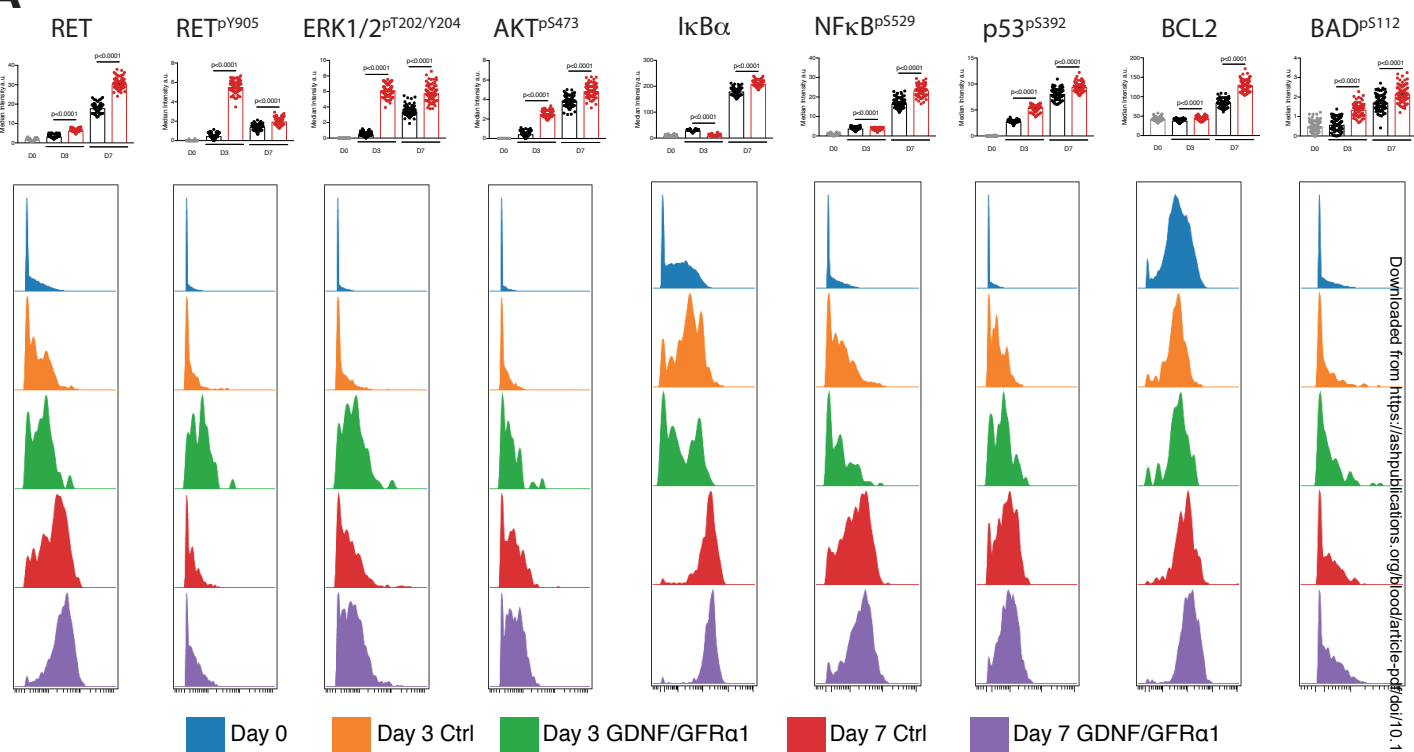


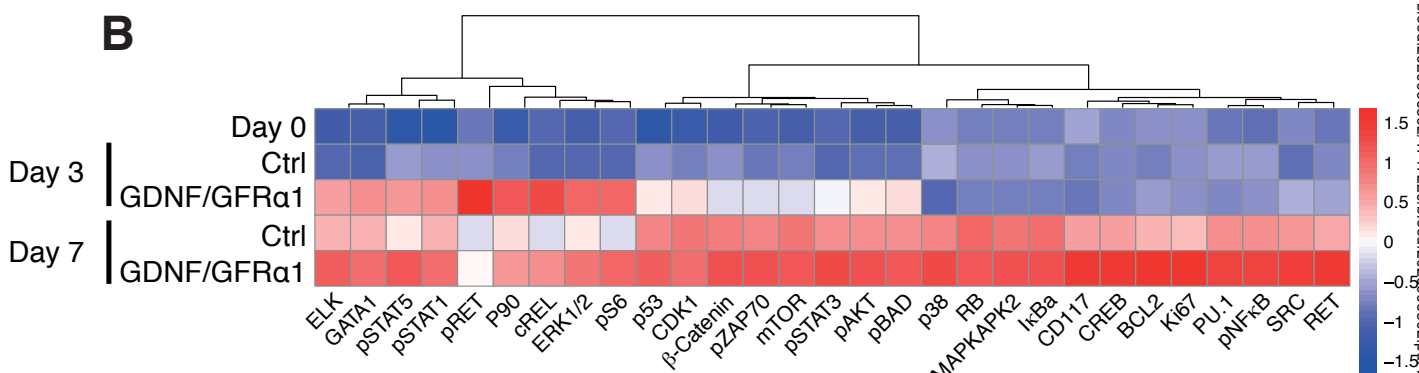
# Figure 5

■ Ctrl  
■ GDNF/GFRα1

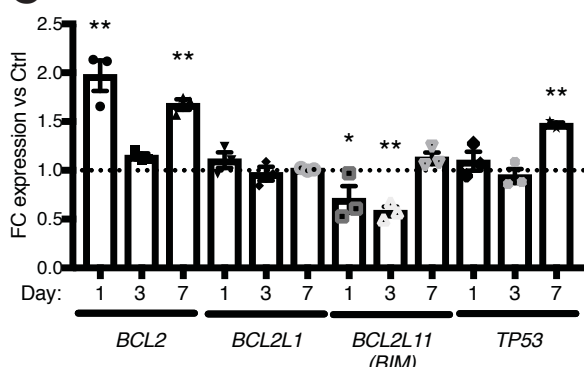
## A



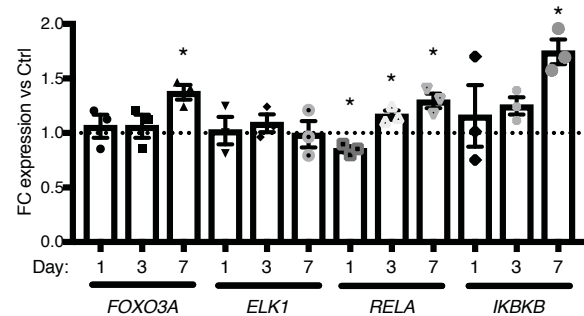
## B



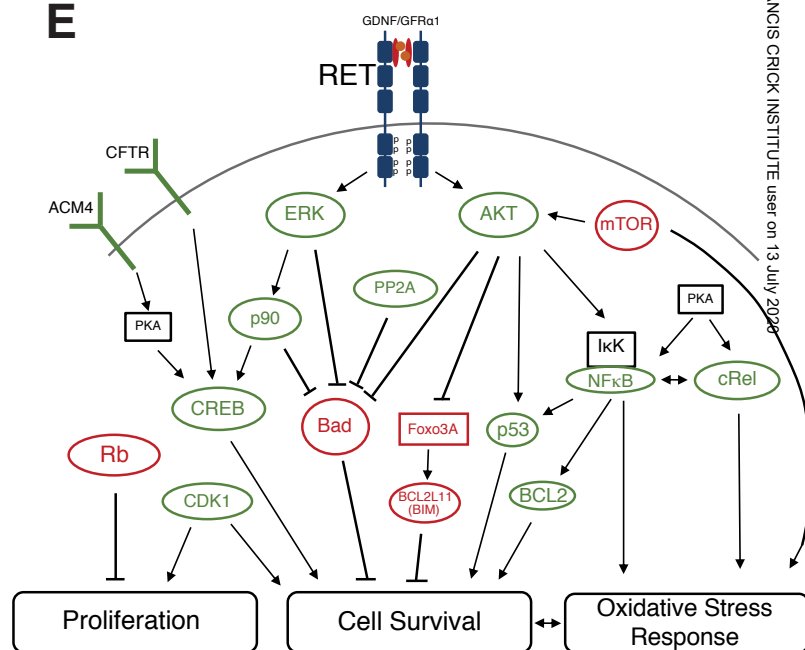
## C



## D



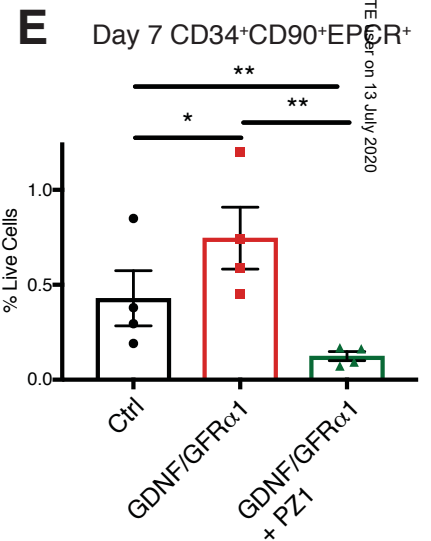
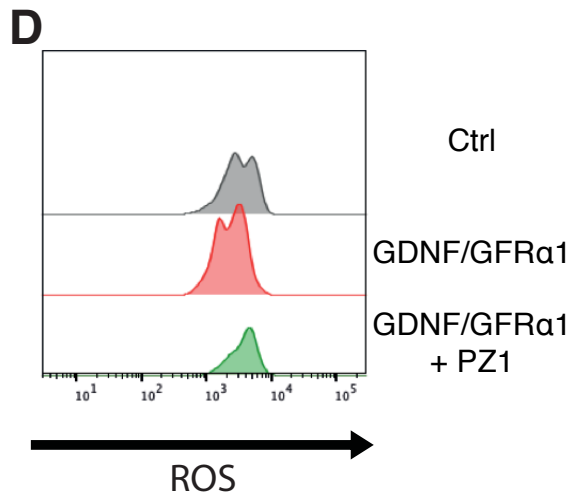
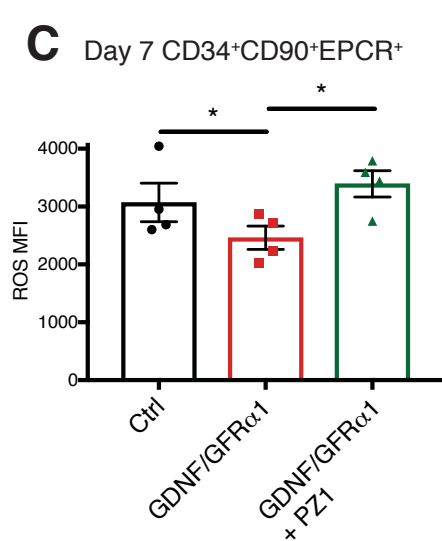
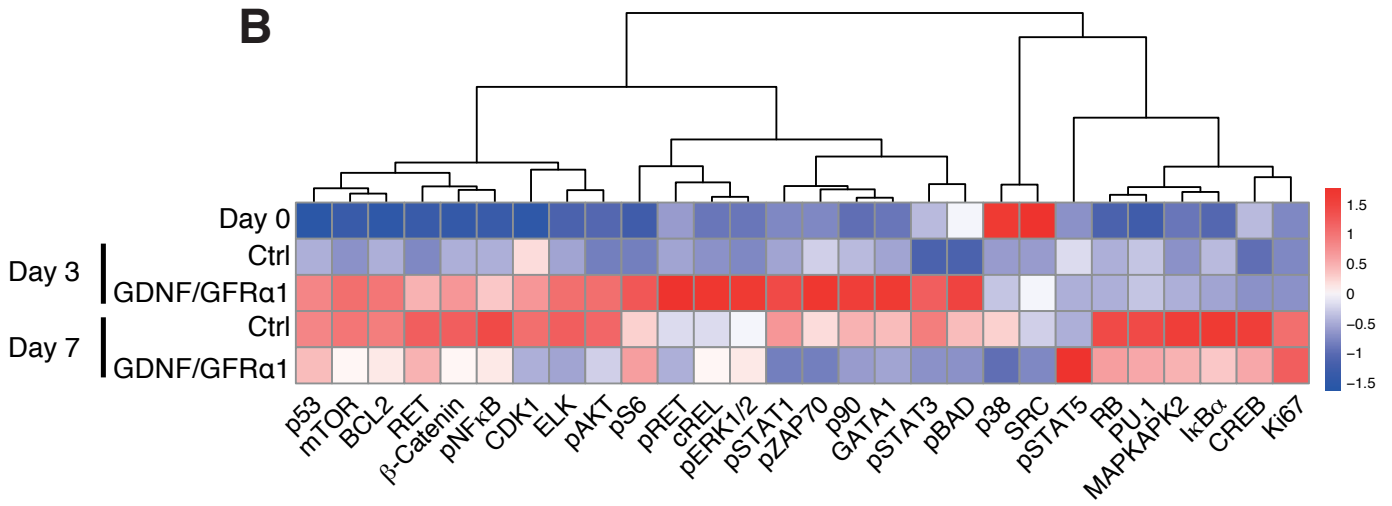
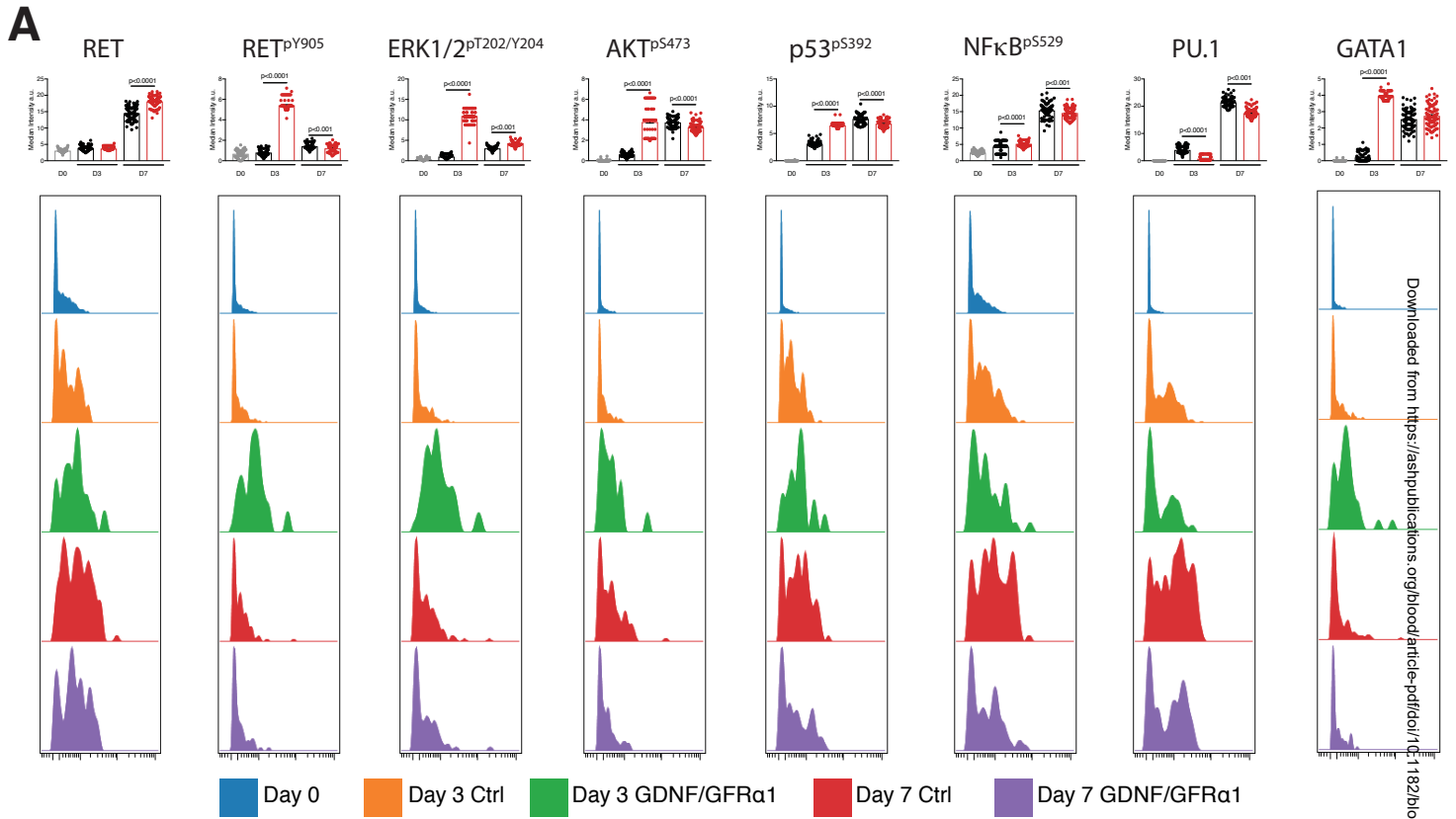
## E



Downloaded from https://ashpublications.org/blood/article-pdf/doi/10.1182/blood.2020063021747220/blood.2020063021.pdf by THE FRANCIS CRICK INSTITUTE user on 13 July 2020

# Figure 6

■ Ctrl  
■ GDNF/GFRα1



Downloaded from https://ashpublications.org/blood/article-pdf/doi/10.1182/blood.2020063027.1747220/blood.2020063027.pdf by THE FRANCIS CRICK INSTITUTE on 13 July 2020